Many-body correlations in shell model effective interactions derived by *ab initio* methods and the $V_{\text{low-k}}$ approach*

Xiao-Bao Wang(王小保)[1)] Guo-Xiang Dong(董国香)[1;1)] Hua-Lei Wang(王华磊)[2] Cen-Xi Yuan(袁岑溪)[3]
Yong-Jing Chen(陈永静)[4] Ya Tu(图雅)[5]

[1] School of Science, Huzhou University, Huzhou 313000, China
[2] School of Physics and Engineering, Zhengzhou University, Zhengzhou 450001, China
[3] Sino-French Institute of Nuclear Engineering and Technology, Sun Yat-Sen University, Zhuhai 519082, China
[4] Key Laboratory of Science and Technology on Nuclear Data, China Institute of Atomic Energy, Beijing 102413, China
[5] School of Physics Science and Technology, Shenyang Normal University, Shenyang 110034, China

Abstract: We investigate many-body correlations caused by two- and three-body (2-, 3bd) forces. Shell-model effective interactions derived from *ab initio* methods (coupled-cluster method, no-core shell model) are adopted. $V_{\text{low-k}}$ potentials, based on many-body perturbation theory, are also tested, especially for their cut-off dependence. We compare the central, tensor and spin-orbit interactions from microscopic theory to the fitted interactions. After the inclusion of the three-body force, the matrix elements become fairly close to those fitted directly to experimental data. Calculations of neutron-rich oxygen isotopes are performed, to clarify the effects of 3bd forces, tensor, and spin-orbit interactions on the nuclear binding and excitation energies. We find that the 3bd force can influence the binding energies greatly, which also determines the drip line position, while its effect on excitation energies is not very pronounced. The spin-orbit force, which is part of the 2bd force, can affect the shell structure explicitly, at least for neutron-rich systems.

Keywords: shell model, effective interactions, tensor force, three-body force

PACS: 21.60.Cs, 21.30.Fe, 21.60.De **DOI:** 10.1088/1674-1137/42/11/114103

1 Introduction

The precision of effective interactions is a critical element for reliable predictions. Microscopic derivations of effective interactions in valence space for the shell model have been studied for decades, since the pioneer work by Gerry Brown and Tom Kuo in 1966. They derived the effective interactions by the reaction-matrix G method, via the sum of particle-particle ladder diagrams from the Hamada-Johnston nucleon-nucleon potential [1, 2]. Many efforts have been made to obtain effective interactions microscopically, which can give precise predictions on nuclear structure properties. To renormalize nuclear potentials into the limited model space, the Wilsonian renormalization group (WRG) method [3], the Lee-Suzuki method [4], the unitary transformation method [5], etc., have been developed. In particular, the renormalization group has been used to obtain the model-independent low momentum nucleon-nucleon interaction $V_{\text{low-k}}$ [6].

On the other hand, understanding nuclear structure properties in a non-perturbative way has been an important objective of theoretical nuclear research for quite a long time. Different types of *ab initio* approach have been developed, e.g. the no-core shell model (NCSM) [7], Green-function-Monte-Carlo method (GFMC) [8], in-medium similarity renormalization group (IM-SRG) method [9], coupled-cluster (CC) method [10], etc. With the increase of computing power, improvements in numerical methods and the progress of microscopic theory, more and more nuclei can now be studied by *ab initio* methods. The heaviest nucleus calculated by an *ab initio* approach to date is ^{48}Ca [11]. In order to compensate for the increasing dimensions of the many-body wave function, the core has to be re-introduced. Thus, non-perturbative effective interactions in valence space have recently been developed. Within the NCSM, attempts have been made to generate the effective interactions in a given valence space by the projection method from the full Hamiltonian [12, 13]. Similarly, the IM-SRG method [14] and CC [15] approach also produce effective interactions for the shell model. The agree-

Received 25 July 2018, Published online 7 September 2018

∗ Supported by National Natural Science Foundation of China (11505056, U1732138, 11605054, 11790325, 11305108, 11575290, 11675148, 11747312, 11775316) and the Outstanding Young Talent Research Fund of Zhengzhou University (1521317002)

1) E-mail: gxdong@zjhu.edu.cn

ment between the shell-model calculations with non-perturbative effective interactions and the results from *ab initio* methods has been tested. Thus, the derivation of non-perturbative effective interactions provides another way to study heavier nuclei starting from first principles.

Previously, we have studied [16–19] the systematics of monopole parts of shell-model effective interactions and their effects on shell evolution. We have also studied the Kuo-Brown interactions, which were the first microscopic interactions derived for the shell model, and compared the non-perturbative interaction from the NCSM with other effective interactions. In the present paper, we study the contribution of the three-body (3bd) force to the effective interactions, by using the non-perturbative effective interactions derived by the CC method from the chiral effective field. We also study the $V_{\text{low-k}}$ interactions from the chiral potential. In particular, we apply two low-momentum on-shell-equivalent potentials which are characterized by different cutoffs. Thus the effect of short-range correlations from different cutoffs can also be seen.

The paper is structured as follows. We introduce the basic concepts in Section 2. In Section 3, we provide the analysis of the effective interactions and perform shell model calculations. Conclusions are drawn in Section 4.

2 Theoretical framework

For finite nuclei with particle number A, the A-body problem is extremely difficult to handle, and a perturbative method is usually adopted, such as

$$\begin{aligned} H^A &= \sum_{i=1}^{A}\frac{p_i^2}{2m}+\sum_{i<j}V_{NN}^{ij}=(T+U)+(V_{NN}-U) \\ &= H_{\text{o}}+H_{\text{res}}, \end{aligned} \tag{1}$$

where V_{NN}^{ij} is the nucleon-nucleon interaction, H_{o} is the unperturbed part of the Hamiltonian, which is supposed to dominate the Hamiltonian (by choosing the auxiliary one-body potential U), and H_{res} is the residual interaction. Such a treatment is used in many-body perturbation theory (MBPT). In the shell model, the effective Hamiltonian H_{SM}^A is further truncated in the valence space, as

$$H_{\text{SM}}^A=H_0+H_1+V_2^A, \tag{2}$$

where H_0 is the interactions of the nucleons in the inert core, H_1 is the one-body part, related to interactions between valence particles and the core nucleons, and V_2^A is the two-body part, for the interactions among valence particles.

For the choice of nuclear potential, the chiral effective potential, which can be traced back to low-energy QCD [20], is becoming more and more popular. It also provides a way to build up the nuclear interactions and currents in a systematic way. In this framework, the three-body force appears naturally at next-to-next-to-leading order (N2LO). For the study of low-energy nuclear physics, a cut-off momentum Λ is chosen so that all fields with momentum greater than Λ are integrated out, and the low momentum interaction $V_{\text{low-k}}$ can be obtained within Λ [21]. Shell-model effective interactions are then further derived by including the perturbation diagrams up to third order in $V_{\text{low-k}}$ by way of the Q-box plus folded-diagram method.

To test the effect of the cutoff dependence of $V_{\text{low-k}}$ interactions, we choose two different cutoffs, 2.0 fm^{-1} and 2.6 fm^{-1}. In Ref. [21] it was found that the cutoff should be larger than $m_{2\pi}\sim$1.4 fm^{-1}. However, it cannot be too large (depending how high E_{lab} is when fitting the NN potentials to the empirical phase shifts). Furthermore, the convergence will become bad with increasing cutoff. In Ref. [22], a cutoff of 2.6 fm^{-1} was used, and the authors stated that such a large cutoff can include more short-range correlations, which can partly absorb the effect of the three-body force. Therefore, we would like to compare the contribution of short-range correlations with the three-body force in the present paper.

G. R. Jansen et al. [23] derived the valence-space effective interactions for the shell model (they call it coupled-cluster effective interactions, CCEI) from the CC method in the singles-and-doubles approximation with Λ-triples correction (Λ-CCSD(T)). CCEI is derived by expanding the original many-body Hamiltonian in a form suitable for the shell model:

$$H_{\text{CCEI}}=H_0^{A_c}+H_1^{A_c+1}+H_2^{A_c+2}, \tag{3}$$

where $H_0^{A_c}$, $H_1^{A_c+1}$, and $H_2^{A_c+2}$ are the core, one-body, two-body, and higher-body valence-cluster Hamiltonians. The chiral potential with two-body force at the level of N3LO and three-body force at N2LO were used for their work. The agreement between shell model calculations with CCEI and Λ-CCSD(T) calculations was tested. They also showed that the results from A-independent CCEI are closer to the results from Λ-CCSD(T) calculations than the A-dependent CCEI. Thus, they have built a shell-model effective interaction for the full valence space (sd shells) based on the CC theory. We use their CCEI in our work, to compare with $V_{\text{low-k}}$ interactions. We also adopt the *ab initio* shell-model interactions from the NCSM [24]. All of these interactions are derived from chiral potentials (N3LO).

The monopole components of the effective interactions [25], which are the angular-momentum averaged two-body matrix elements, can have a dominating effect on the shell evolution. They can be given as,

$$V(jj';T)=\frac{\sum_J(2J+1)V(jj'jj';JT)}{\sum_J(2J+1)}, \tag{4}$$

where the summations run over all Pauli-allowed values of the angular momentum J.

We also use the spin-tensor decomposition method [26–29] to decompose the two-body-matrix-elements (TBMEs) of the effective interactions into central force, tensor force, and spin-orbit force. Since shell model effective interactions are valence-space truncated, a special spin-orbit interaction called the anti-symmetric spin-orbit force (ALS) can occur, which can break the relative parity in the TBMEs. The possible origins of ALS are core polarization, high-order terms of perturbations or three-body forces [30, 31]. A strong ALS component may indicate large contributions from the 3bd force or high-order perturbations.

3 Calculations and discussion

To study the systematics of microscopic methods, we adopt the effective interactions derived by *ab initio* methods, *i.e.* the CC method [23] and the NCSM [24]. The $V_{\text{low-k}}$ interaction is calculated by the MBPT code [32], and used here for comparison. In these microscopic methods, the same chiral potential is accepted (two-bode (2bd) force at the level of N3LO and 3bd force at the level of N2LO). Takaharu Otsuka et al. [33] have proved that the 3bd force can have a large impact on neutron-rich nuclei. Especially, they showed that the microscopic description of the drip line of neutron-rich oxygen isotopes can only be given correctly by the 3bd force.

We will focus on the neutron-neutron parts of effective interactions in the present paper (in the following parts, all the effective interactions are for neutron-neutron parts only). All the effective interactions are for the *sd*-shells. We also use USDB interactions in this work. The USDB interaction has been optimized from fitting to experimental data by the linear combination method [34]. Thus, it can be seen as "pseudo" experimental data (this kind of interaction is also called an empirical interaction in the literature). We will test the contributions of the 3bd force to the TBMEs and monopole components of shell-model interactions. The cutoff dependence from $V_{\text{low-k}}$ interactions will also be studied, and the short-range correlations compared with the 3bd force.

First, we study the systematics of TBMEs directly. As shown in Fig. 1, we have compared the TBMEs of several effective interactions to those from the $V_{\text{low-k}}$ approach with cutoff 2.0 fm^{-1}. In the figure, all the TBMEs with 2bd force only are fairly close to each other, independent of the microscopic methods. 2bd and 3bd forces have been included in the effective interactions (CCEI) derived by the CCSD(T) calculation [23]. It can be seen that most TBMEs from CCEI are less attractive than the interactions with 2bd force only. The CCEI is much closer to the USDB interaction ("pseudo" experimental data). Thus, the 3bd force is a necessary component for the effective interaction.

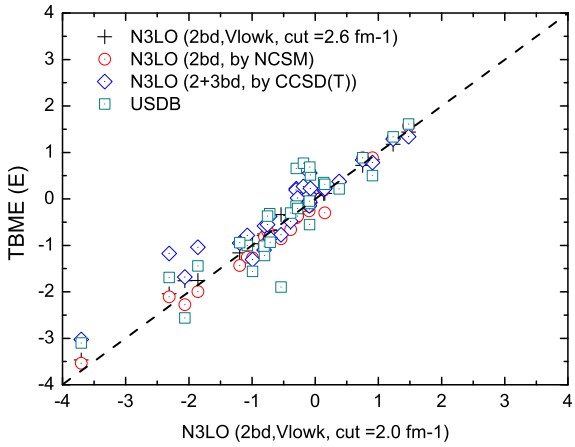

Fig. 1. (color online) Different sets of TBMEs are compared to those derived by the $V_{\text{low-k}}$ approach with cutoff 2.0 fm^{-1}. The TBMEs derived by the NCSM, those from the $V_{\text{low-k}}$ approach with cutoff 2.6 fm^{-1}, and those derived from CCSD(T) calculations are shown. The former two interactions are derived with 2bd force only, and the last one includes 2bd and 3bd forces. TBMEs from USDB are also included for comparison.

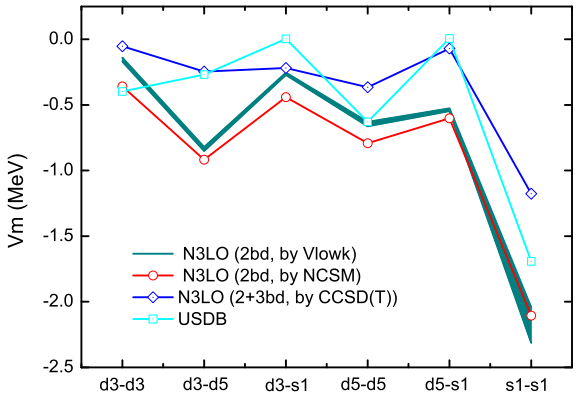

Fig. 2. (color online) The monopole parts of the effective interactions. The monopole elements of the NCSM (2bd force only) and CCSD(T) method (2+3 body force), and USDB interactions are shown. The monopole strength from $V_{\text{low-k}}$ interactions with the cutoff in the range of 2.0 fm^{-1} to 2.6 fm^{-1} is plotted as a shaded area (the strength with cutoff 2.0 fm^{-1} is more attractive).

Second, we compare the monopole components of these effective interactions, as shown in Fig. 2. The monopole terms in the $V_{\text{low-k}}$ approach with different cutoffs are shown as a shaded area. More information from short-range correlations (the high momentum part of NN interactions) is included when one increases the

cutoff of $V_{\text{low-k}}$ interactions. However, in the range of Λ=2.0$\sim$2.6 fm^{-1}, the monopole elements of the $V_{\text{low-k}}$ interactions are systematically more attractive than those of the USDB interaction. Thus, the so-called monopole defects cannot be cured by the tuning of the cutoff in $V_{\text{low-k}}$ interactions. The variances between the interactions with different cutoffs are not very large, except for the monopole term between $s1/2$ orbitals. The monopole interactions from NCSM are also very similar to those from the $V_{\text{low-k}}$ approach. Only after the explicit inclusion of the 3bd force does the monopole elements become close to the empirical values (monopole strength of USDB).

The central, tensor, ALS and LS forces in these monopole elements are shown in Figs. 3(a-d) respectively. From Fig. 3(a), it can be seen that the curves of the monopole components contributed by the central force are nearly parallel to each other. Again, the strength of the central force derived by the NCSM is very close to that obtained by the $V_{\text{low-k}}$ approach. As shown in the figure, the 3bd force gives a strong repulsive contribution to the central interactions, and by including the 3bd force, the monopole terms from the central force are very close to those of the empirical interaction USDB. By increasing the cutoff Λ in the $V_{\text{low-k}}$ approach, more short-range correlations can be absorbed into the effective interactions, so the resulting monopole components with cutoff 2.6 fm^{-1} can be more repulsive than those with the cutoff 2.0 fm^{-1}. However, it can be seen in the figure that this effect from increasing the cutoff is much smaller than that from the inclusion of the 3bd force. Since the central force gives large contributions to the binding energy of nuclei, it can be expected that the contributions from the 3bd force to the binding energy are also large through the channel of central interaction.

In Fig. 3(b), the monopole components of the tensor force are given. The N3LO potential (2bd force) has a strong tensor channel, and it is reduced by the 3bd forces. The tensor force is weak in the empirical interaction. Figure 3(c) shows the ALS force. The empirical interaction has a strong ALS component. The microscopic interactions with 2bd force only have a weak ALS force, no matter whether the interactions are derived by the $V_{\text{low-k}}$ method or NCSM. It can be seen that the 3bd force has increased the ALS force explicitly, so that the resulting ALS components have become quite close to those in the empirical interaction. In Fig. 3(d), it is seen that LS force has the smallest contributions to the monopole terms, and its strength is quite uncertain.

In Figs. 3(b-d) one can also find that in these non-central interactions, the effective interactions by the $V_{\text{low-k}}$ approach with different cutoffs are very close. Thus, the short-range correlations in the 2bd force mainly affect the effective interactions through the channel of the central interaction.

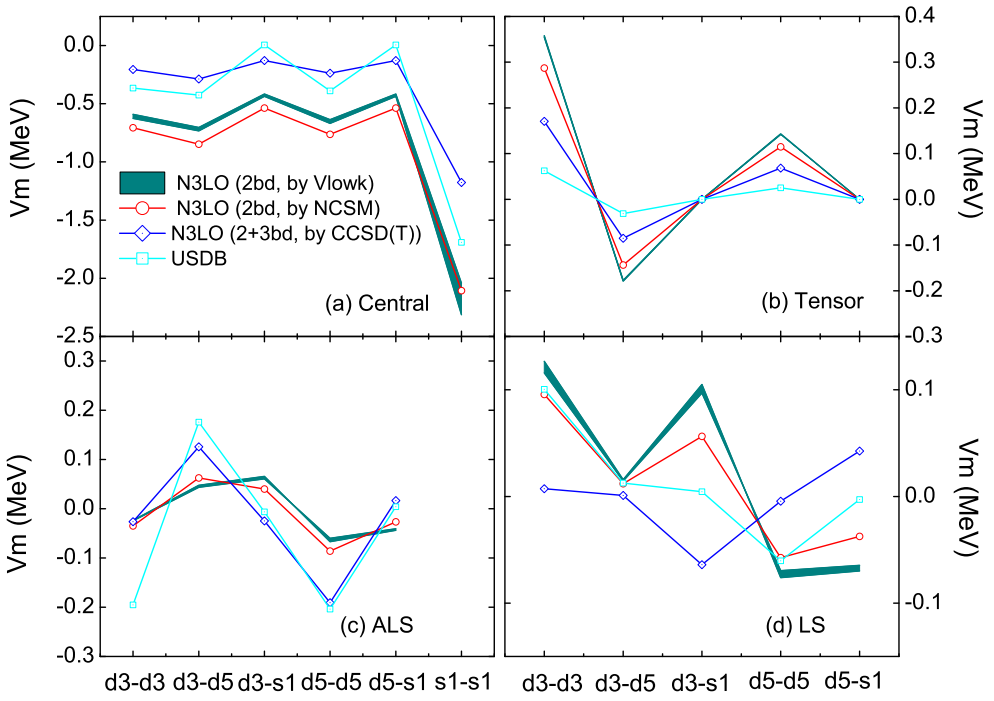

Fig. 3. (color online) The central, tensor, ALS and LS force of the effective interactions. The NCSM (2bd force only) and CCSD(T) method (2+3 body force), and USDB interactions are shown. The strength from $V_{\text{low-k}}$ interactions with the cutoff in the range of 2.0 fm^{-1} to 2.6 fm^{-1} is plotted as a shaded area (the strength with cutoff 2.0 fm^{-1} is more attractive).

We then do shell-model calculations to study how the different components of effective interactions influence the nuclear properties. The neutron-rich oxygen isotopes are chosen for the test of neutron-neutron interactions. The binding and excitation energies are calculated, as shown in Figs. 4 and 5, respectively. These two observables can reflect important features of effective interactions. To study how different components in effective interactions, especially the 3bd force, tensor force, ALS force, and LS force, affect the shell structure, we use five sets of effective interactions: the complete interaction with 2bd plus 3bd forces (derived by the CCSD(T) method), the interaction without the 3bd force, the interaction without the tensor force, the interaction without the ALS force, and the interaction without the LS force. Through comparison of the results with the complete and incomplete interaction, one can see the effects of different components directly. In this work, we only study the effects from the two-body effective interactions. When we do these calculations, the single particle energies are fixed to the original values derived by the CCSD(T).

In Fig. 4(a), one can see that the discrepancies between the results with 2bd plus 3bd forces and those with the 2bd force only are large, and increase with the adding of neutrons. Thus, the 3bd force is necessary for the correct description of the binding energies, especially for neutron-rich systems. Also, it can be seen clearly in the figure that one has to include the 3bd force to give a correct drip-line position. Using the effective interaction with the 2bd force only, ^{26}O is still bound. After the inclusion of the 3bd force, ^{24}O is bound and ^{26}O becomes unbound, consistent with experimental data. The calculated binding energy of ^{26}O is less bound than the experimental values. The reason might be that the continuum effect cannot be taken into account properly in the framework of the shell model. In Ref. [35], by considering the continuum effect and 3bd force in the CC method, the binding energy of ^{26}O is more consistent with the experimental data.

In Fig. 4(b), the calculation results of binding energies using the effective interaction with and without tensor force are very close. This may indicate that for the neutron-rich nuclei, while the neutron-neutron interaction dominates, the tensor force has a small contribution to the binding energies. By comparing the results in Fig. 4(c) with those in Figs. 4(a) and (b), one can find that the ALS force has a more explicit effect on binding energy than the tensor force but a smaller contribution than the 3bd force. In Fig. 4(d), it is seen that LS force can also influence the binding energies explicitly. However, for this neutron-rich isotope chain, its contribution to the binding energy is like a simple shift, and the shell structure is not changed much by the LS force. Thus, from this picture, one can learn that the 3bd force is most essential for the binding energies.

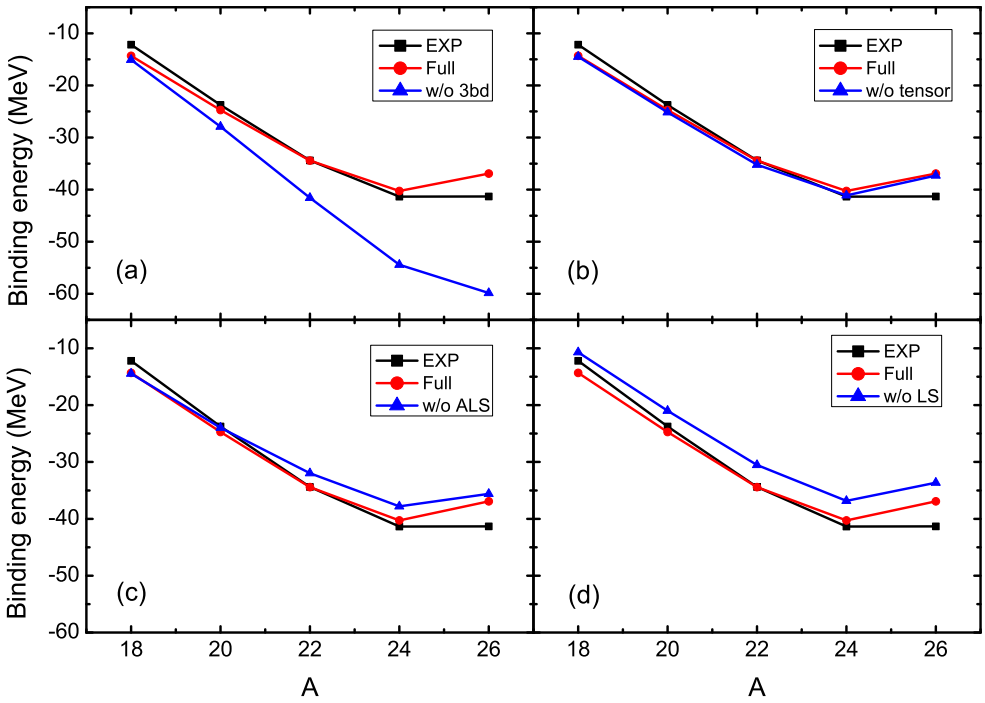

Fig. 4. (color online) Ground-state energies for the oxygen isotopes, relative to ^{16}O by using different sets of interaction. 2bd plus 3bd forces (derived by the CCSD(T) method), the interaction without the 3bd force, the interaction without the tensor force, the interaction without the ALS force, and the interaction without the LS force are labeled as "Full", "w/o tensor", "w/o ALS" and "w/o LS" respectively.

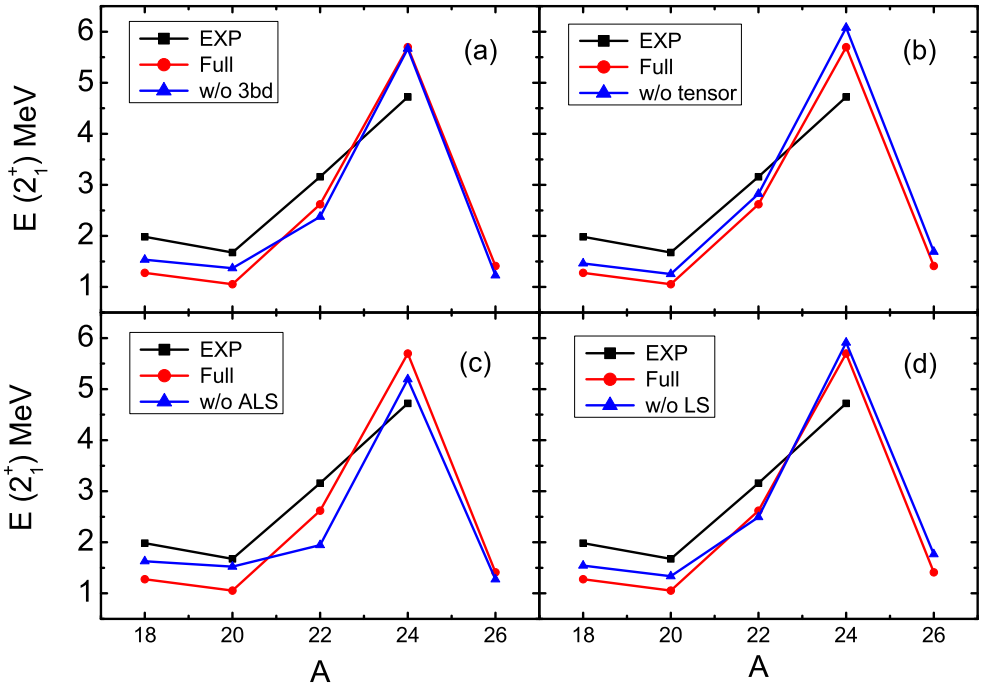

Fig. 5. (color online) The first 2^+ excitation energies for the oxygen isotopes, relative to ^{16}O by using different sets of interaction. 2bd plus 3bd forces (derived by the CCSD(T) method), the interaction without the 3bd force, the interaction without the tensor force, the interaction without the ALS force, and the interaction without the LS force are labeled as "Full", "w/o tensor", "w/o ALS" and "w/o LS" respectively.

The results for the excitation energies are shown in Fig. 5. In this case, the 3bd force has a less pronounced effect. Thus, as for the excitation energies, which are energies relative to the ground state, we may still have a good calculation without the explicit inclusion of the 3bd force. The effect from the tensor force is stronger than the LS force, but weaker than the 3bd force and ALS force. In particular, the magic gap at $N=14$ for the oxygen isotope can only be given by the ALS force. In Fig. 5(c), the first 2^+ states are about the same for $^{18-22}$O, for the interaction without ALS. After the inclusion of ALS, the first 2^+ excitation energy of ^{22}O ($N=14$) becomes higher, comparable to the experimental data. The ALS force, as one special component in the two-body spin-orbit interaction, exists in the shell model mostly because of the valence-space truncation. It can be traced back to the core polarization, higher order perturbations, and 3bd forces [30, 31]. Thus, the importance of the ALS components can be seen as the indicator of those many-body correlations.

4 Summary and conclusion

We have studied the effective interactions derived from chiral effective field theory by different microscopic methods. We have used the interactions from the $V_{\text{low-k}}$ approach with different cutoffs and the NCSM and CC theory *ab initio* methods .

We have learned that the discrepancies between the interactions using the same potential from different methods are not very large. The 3bd force can greatly improve the precision of effective interactions. The interaction with 2bd and 3bd forces is very close to the empirical interaction which is fitted from experimental data. The central and non-central monopole elements of these effective interactions were compared, and it was found that the 3bd force can change the central interaction quite a lot. For the neutron-neutron interaction, the 3bd force reduces the strength of the tensor force and increases the spin-orbit (ALS) interaction.

We have also studied the binding and excitation energies of the oxygen isotopes. The 3bd force is essential for the description of the nuclear binding energy. The ALS interaction can have a larger effect than the tensor force. Especially, for the description of the magic gap of $N=14$ in oxygen isotopes, ALS plays an important role. Since the ALS force mostly originates from the 3bd force, it can be seen as another indicator for the importance of the 3bd force and other many-body correlations absorbed by the mapping from full-space CCSD(T) calculations into the truncated model space.

References

1 T. T. S. Kuo, G. E. Brown, Nucl. Phys., **85**: 40–86 (1966)
2 T. T. S. Kuo, G. E. Brown, Nucl. Phys. A, **114**: 241–279 (1968)
3 S. X. Nakamura, Prog. Theor. Phys., **114**: 77–115 (2005)
4 S. Y. Lee, K. Suzuki, Phys. Lett. B, **91**: 173–176 (1980)
5 E. Epelbaum, W. Glöckle, U. G. Meißner, Phys. Lett. B, **439**: 1–5 (1998)
6 S. K. Bogner, T. T. S. Kuo, and A. Schwenk, Phys. Rep., **386**: 1–27 (2003)
7 B. R. Barrett, P. Navratil, and J. P. Vary, Prog. Part. Nucl. Phys., **69**: 131 (2013)
8 J. Carlson and R. Schiavilla, Rev. Mod. Phys., **70**: 743 (1998); J. Carlson, S. Gandolfi, F. Pederiva, Steven C. Pieper, R. Schiavilla, K. E. Schmidt, and R. B. Wiringa, Rev. Mod. Phys., **87**: 1067 (2015); D. Lonardoni, J. Carlson, S. Gandolfi, J. E. Lynn, K. E. Schmidt, A. Schwenk, and X. B. Wang, Phys. Rev. Lett., **120**: 122502 (2018)
9 H. Hergert, S. K. Bogner, T. D. Morris, A. Schwenk, and K. Tsukiyama, Physics Reports, **621**: 165 (2016)
10 G. Hagen, T. Papenbrock, M. Hjorth-Jensen, and D. J. Dean, Rep. Prog. Phys., **77**: 096302 (2014)
11 G. Hagen, A Ekström, Forssén et al, Nature Physics, **12**: 186–190 (2016)
12 A. F. Lisetskiy, B. R. Barrett, M. K. G. Kruse, P. Navrátil, I. Stetcu, and J. P. Vary, Phys. Rev. C, **78**: 044302 (2008)
13 A. F. Lisetskiy, M. K. G. Kruse, B. R. Barrett, P. Navrátil, I. Stetcu, and J.P. Vary, Phys. Rev. C, **80**: 024315 (2009)
14 S. K. Bogner, H. Hergert, J. D. Holt, A. Schwenk, S. Binder, A. Calci, J. Langhammer, and R. Roth, Phys. Rev. Lett., **113**: 142501 (2014)
15 G. R. Jansen, J. Engel, G. Hagen, P. Navrátil, and A. Signoracci, Phys. Rev. Lett., **113**: 142502 (2014)
16 X. B. Wang, G. X. Dong, F. R. Xu, Eur. Phys. J. Web of Conferences, **66**: 02108 (2014)
17 X. B. Wang, G. X. Dong, Sci. China-Phys Mech. Astron., **58**: 102001 (2014)
18 X. B. Wang, G. X. Dong, J Phys. G: Nucl. Part. Phys., **42**: 125101 (2015)
19 X. B. Wang, G. X. Dong, Q. F. Li, C. W. Shen, and S. Y. Yu, Sci. China-Phys. Mech. Astron., **59**: 692011 (2016)
20 R. Machleidt, D. R. Entem, Phys. Rep., **503**: 1 (2011)
21 S. Bogner, T. T. S. Kuo, L. Coraggio, A. Covello, and N. Itaco, Phys. Rev. C, **65**: 051301(R) (2002)
22 L. Coraggio1, A. Gargano, N. Itaco, JPS Conf. Proc., **6**: 020046 (2015)
23 G. R. Jansen, M. D. Schuster, A. Signoracci et al, Phys. Rev. C, **94**: 011301(R) (2016)
24 E. Dikmen, A. F. Lisetskiy, B. R. Barrett, P. Maris, A. M. Shirokov, and J. P. Vary, Phys. Rev. C, **91**: 064301 (2015)
25 R. K. Bansal, J. B. French, Phys. Lett., **11**: 145–148 (1964)
26 J. P. Elliott, A. D. Jackson, H. A. Mavromantis et al, Nucl. Phys. A, **121**: 241–278 (1968)
27 M. W. Kirson, Phys. Lett. B, **47**: 110–114 (1973)
28 K. Yoro, Nucl. Phys. A, **333**: 67–76 (1980)
29 K. Yoshinada, Phys. Rev. C, **26**: 1784–1786 (1982)
30 B. A. Brown, W. A. Richter, R. E. Julies, and B. H. Wildenthal, Annals of Physics, **182**: 191 (1988)
31 K. Yoshinada, Phys. Rev. C, **26**: 1784 (1982)
32 M. Hjorth-Jensen, T. T. S. Kuo, and E. Osnes, Phys. Rep., **261**: 125 (1995); https://github.com/ManyBodyPhysics/ManybodyCodes/
33 T. Otsuka, T. Suzuki, J. D. Holt, A. Schwenk, and Y. Akaishi, Phys. Rev. Lett., **105**: 032501 (2010)
34 B. A. Brown, Phys. Rev. C, **74**: 034315 (2006)
35 G. Hagen, M. Hjorth-Jensen, G. R. Jansen et al, Phys. Rev. Lett., **108**: 242501 (2012)